3-(4-Aroyl-1-methyl-1*H*-pyrrol-2-yl)-*N*-hydroxy-2-propenamides as a New Class of Synthetic Histone Deacetylase Inhibitors. 3. Discovery of Novel Lead Compounds through Structure-Based Drug Design and Docking Studies[†,Δ]

Rino Ragno,*[,‖] Antonello Mai,*[,§] Silvio Massa,[⊥] Ilaria Cerbara,[§] Sergio Valente,[§] Patrizia Bottoni,[⊗] Roberto Scatena,[⊗] Florian Jesacher,[‡] Peter Loidl,[‡] and Gerald Brosch*[,‡]

Dipartimento di Studi di Chimica e Tecnologia delle Sostanze Biologicamente Attive, Università degli Studi di Roma "La Sapienza", P. le A. Moro 5, 00185 Roma, Italy, Dipartimento di Studi Farmaceutici, Università degli Studi di Roma "La Sapienza", P. le A. Moro 5, 00185 Roma, Italy, Dipartimento Farmaco Chimico Tecnologico, Università degli Studi di Siena, via A. Moro, 53100 Siena, Italy, Istituto di Biochimica e Biochimica Clinica, Università Cattolica del Sacro Cuore, L.go F. Vito 1, 00168 Roma, Italy, and Department of Molecular Biology, University of Innsbruck, Medical School, Peter-Mayr-Strasse 4b, 6020 Innsbruck, Austria

Received September 18, 2003

Aroyl-pyrrole-hydroxy-amides (APHAs) are a new class of synthetic HDAC inhibitors recently described by us. Through three different docking procedures we designed, synthesized, and tested two new isomers of APHA lead compound 3-(4-benzoyl-1-methyl-1*H*-pyrrol-2-yl)-*N*-hydroxy-2-propenamide (**1**), compounds **3** and **4**, characterized by different insertions of benzoyl and propenoylhydroxamate groups onto the pyrrole ring. Biological activities of **3** and **4** were predicted by computational tools up to 617-fold more potent than that of **1** against HDAC1; thus, **3** and **4** were synthesized and tested against both mouse HDAC1 and maize HD2 enzymes. Predictions of biological affinities (K_i values) of **3** and **4**, performed by a VALIDATE model (applied on either SAD or automatic DOCK or Autodock results) and by the Autodock internal scoring function, were in good agreement with experimental activities. Ligand/receptor positive interactions made by **3** and **4** into the catalytic pocket, in addition to those showed by **1**, could at least in part account for their higher HDAC1 inhibitory activities. In particular, in mouse HDAC1 inhibitory assay **3** and **4** were 19- and 6-times more potent than **1**, respectively, and **3** and **4** antimaize HD2 activities were 16- and 76-times higher than that of **1**, **4** being as potent as SAHA in this assay. Compound **4**, tested as antiproliferative and cytodifferentiating agent on MEL cells, showed dose-dependent growth inhibition and hemoglobin accumulation effects.

Introduction

Histone deacetylase (HDAC) and histone acetyltransferase (HAT) enzymes are involved in determining the acetylation status of histones, and such reversible acetylation reactions play an important role in modulation of chromatin topology and regulation of gene expression. Histones H2A, H2B, H3, and H4 exhibit acetyl groups at the ϵ-amino-terminal lysine residues within the tails extending from the histone octamer of the nucleosome core. Among them, histones H3 and H4 constitute the main targets of HDAC enzymatic activity.[1−3] Gene transcription or repression is associated with the ability of transcriptionally competent genes to recruit either HAT or HDAC proteins to the promoter. HAT-promoted acetylation activity is related with nucleosomal relaxation and gene transcription, while HDAC-promoted deacetylation produces a tightness of nucleosomal integrity and gene silencing.[4−6]

Aberrant acetylation of histone tails emerging either from HAT mutations or abnormal recruitment and/or overexpression of HDACs have been clearly linked to carcinogenesis. Inappropriate HDAC-mediated transcriptional repression is a common molecular mechanism used by oncoproteins to produce alterations in chromatin structure and blockage of normal cell differentiation. Compounds able to inhibit HDAC activity (HDAC inhibitors, such as trichostatin A (TSA),[7] trapoxin,[8] HC-toxin,[9] apicidin,[10] suberoylanilide hydroxamic acid (SAHA),[11] cyclic hydroxamic acid-containing peptides (CHAPs),[12,13] FK-228,[14] MS-275,[15,16] sodium valproate[17,18]) can reactivate gene expression, and they are potent inducers of growth arrest, differentiation, or apoptotic cell death in a variety of transformed cells in culture and in tumor-bearing animals.[19−21]

In 1999 the X-ray crystal structure of the catalytic core of a bacterial HDAC homologue (histone deacetylase-like protein, HDLP)[22] revealed the binding mode

* To whom correspondence should be addressed. A.M., Tel.: +396-4991-3392; Fax: +396491491; e-mail: antonello.mai@uniroma1.it. (Molecular modeling): R.R., Tel.: +396-4991-3152. Fax: +396491491; e-mail: rino.ragno@uniroma1.it. (Biology): G.B., Tel.: 0512-507-3608; Fax: 0512-507-2866; e-mail: gerald.brosch@uibk.ac.at.

† Part 2: Mai, A.; Massa, S.; Cerbara, I.; Valente, S.; Ragno, R.; Bottoni, P.; Scatena, R.; Loidl, P.; Brosch, G. 3-(4-Aroyl-1-methyl-1*H*-2-pyrrolyl)-*N*-hydroxy-2-propenamides as a New Class of Synthetic Histone Deacetylase Inhibitors. 2. Effect of Pyrrole C2 and/or C4 Substitutions on Biological Activity. *J. Med. Chem.*, in press.

Δ Dedicated to Prof. Marino Artico on the occasion of his 70th anniversary.

‖ Dipartimento di Studi di Chimica e Tecnologia delle Sostanze Biologicamente Attive, Università degli Studi di Roma "La Sapienza".

§ Dipartimento di Studi Farmaceutici, Università degli Studi di Roma "La Sapienza".

⊥ Università degli Studi di Siena.

⊗ Università Cattolica del Sacro Cuore, Roma.

‡ University of Innsbruck.

10.1021/jm031036f CCC: $27.50
Published on Web 02/10/2004

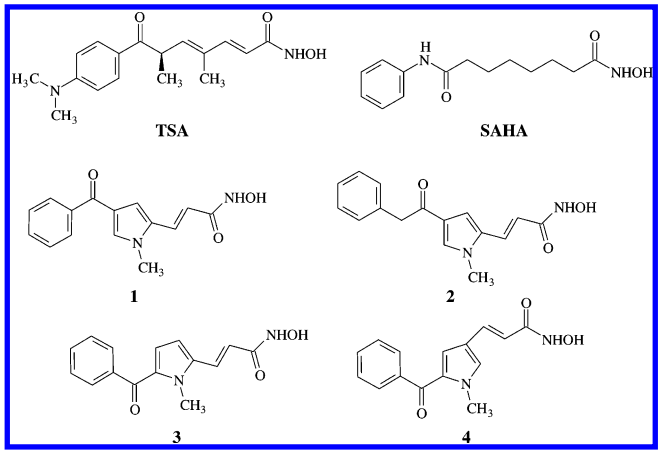

Figure 1. Chemical Structures of TSA, SAHA, and APHA compounds.

of TSA and SAHA (Figure 1) into the enzyme catalytic pocket. Prompted by these data, we performed three-dimensional (3D) structure-based design and molecular modeling studies on pyrrole-containing TSA analogues previously synthesized by us as antimicrobial agents.[23,24] Since the predicted pK_i values of such compounds complexed with HDLP were in the low (or sub-) micromolar range,[25] we tested the pyrrole derivatives against maize histone deacetylase HD2,[26] obtaining IC_{50} values at low micromolar concentrations (IC_{50} values = 1.9−4.0 μM).[25] A refinement of binding mode of the aroylpyrrolyl-hydroxy-amide (APHA) lead compound **1** (Figure 1) in the deacetylase core was obtained by using a virtual HDAC1 catalytic pocket modeled from HDLP coordinates.[27] Chemical manipulations[28,29] performed on various portions of the **1** skeleton yielded a new molecule, *N*-hydroxy-3-(1-methyl-4-phenylacetyl-1*H*-pyrrol-2-yl)-2-propenamide **2** (Figure 1), which was 38-fold more potent than **1** in inhibiting HD2 in vitro.[28] Such improvement of biological activity was partially clarified by inspection of the **2** binding mode into the modeled HDAC1 coordinates. The higher flexibility of the pyrrole C_4-phenylacetyl moiety of **2** respect to that of the C_4-benzoyl substituent of **1**, joined with a more favorable repositioning of the pyrrole *N*-methyl group into the deacetylase pocket, can almost in part account for the enhancement of inhibiting activity observed from **1** to **2**.[28]

In parallel with such studies, we applied a different approach on the **1** structure to discover novel leads, using structure-based drug design and docking procedures. Particularly, we designed two isomers of **1**, 3-(2-benzoyl-1-methyl-1*H*-pyrrol-5-yl)-*N*-hydroxy-2-propenamide **3** and 3-(2-benzoyl-1-methyl-1*H*-pyrrol-4-yl)-*N*-hydroxy-2-propenamide **4** (Figure 1), and we performed computational studies to predict their HDAC inhibiting activity. As the predicted pK_i values were in the submicromolar range, we synthesized **3** and **4**, and tested them against both maize HD2 and mouse HDAC1 enzymes. Moreover, antiproliferative and cytodifferentiating activities of **4** on Friend murine erythroleukemia (MEL) cells were also determined.

Docking Studies Performed on 3 and 4 into the Modeled HDAC1 Catalytic Core. Prediction of HDAC1 Inhibiting Activity. In the chemical structure of the APHA lead compound **1**, virtual rotation of *N*-methylpyrrole ring between benzoyl and *N*-hydroxy-2-propenamide moieties allowed us to design two isomers of **1**, 3-(2-benzoyl-1-methyl-1*H*-pyrrol-5-yl)-*N*-hydroxy-2-propenamide **3** and 3-(2-benzoyl-1-methyl-1*H*-pyrrol-4-yl)-*N*-hydroxy-2-propenamide **4** (Figure 1). Extensive binding mode analyses were undertaken to see if the HDAC1 enzyme inhibitory potency would be influenced by the above different rearrangement of benzoyl and *N*-hydroxypropenamide substituents on the pyrrole ring.

Table 1. VALIDATE and Autodock Predicted Anti-HDAC1 pK_i Compared with Experimental pIC_{50} Values of APHA Isomers **1**, **3**, **4**, and TSA, and SAHA

	predicted pK_i				experimental pIC_{50}	
	VALIDATE					
compd	SAD	DOCK	Autodock	Autodock	HDAC1	HD2
3	5.87	7.31	7.76	5.29	6.64	6.60
4	7.13	7.55	7.47	5.73	6.11	7.30
1	5.76[27]	4.76[28]	7.31[28]	5.65[28]	5.31[27]	5.42[27]
TSA	8.61[a,27]	7.26[28]	7.92[28]	7.41[28]	8.70[27]	8.15[27]
SAHA	6.69[a,27]	6.79[28]	7.15[28]	6.21[28]	6.95[27]	7.30[27]

[a] Predicted from X-ray experimental data.[22]

Table 2. Minimized Complex Steric Energies (kJ/mol) (AMBER force field) Relative to APHA Isomers **3** and **4** Obtained by DOCK, Autodock, and SAD Procedures into the Modeled HDAC1. For Direct Comparison the Same Values for **1**, TSA, and SAHA Are Reported

docking method	**3**	**4**	**1**[a]	TSA[a]	SAHA[a]
DOCK	−7754.958	−7710.129	−7174.81	−8909.93	−7369.18
Autodock	−8737.534	−10161.400	−8913.90	−9976.13	−10363.13
SAD	−8581.698	−8457.775	−7828.92	ND[b]	ND[b]

[a] Reference 28. [b] ND, not determined.

Initially, binding mode analyses of **3** and **4** into the modeled HDAC1 structure were investigated using a semiautomatic dock (SAD) procedure, analogous to that reported for **1**.[27] In parallel experiments, docking studies were performed on **3** and **4** structures by the mean of the DOCK 4.0.2[30] and Autodock 3.0.5[31] programs. The results of the automatic docking procedures (DOCK and Autodock) were energy rescored by a single point minimization by the MACROMODEL molecular mechanics program,[32] using the AMBER all atom force fields[33,34] and point charges calculated with the MOZYME routine as implemented in the MOPAC2000 program[35,36] (see Experimental Section).

From docking studies three bound conformations for both **3** and **4** were obtained, and their associated HDAC inhibitory potencies, expressed as pK_i values, were predicted using our in house refined VALIDATE scoring function model.[37] In Table 1 the pK_i prediction values for APHA isomers **3** and **4** compared with their experimental pIC_{50} values (see below) are reported. For comparison purpose, **1**, TSA, and SAHA pK_i prediction values are also shown.

Among the minimized ligand/HDAC1 complexes, the most stable ones were those proposed by Autodock (Table 2).

Similarly as previously observed,[28] DOCK and Autodock results were in good agreement each other and with those obtained by the SAD procedure (Table 3).

To compare the docked molecules (**1**, **3**, **4**, TSA, and SAHA), their binding conformations obtained by Autodock are depicted in Figure 2.

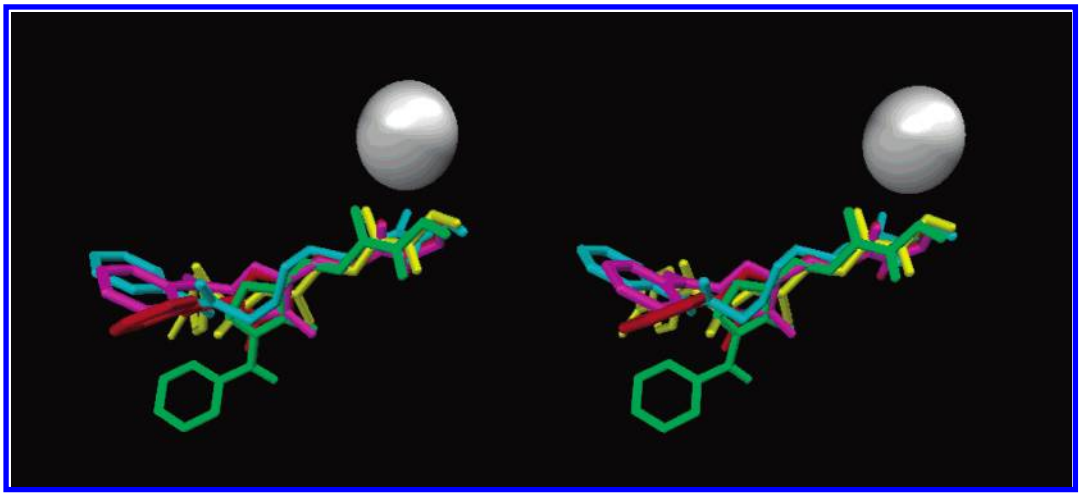

Figure 2. Stereoview of superimposition of the Autodock docked conformations of **1** (magenta), **3** (green), **4** (red), TSA (yellow), and SAHA (cyan). The gray ball represents the mean position of the zinc ion. HDAC1 pocket and nonessential hydrogen atoms are not shown for the sake of clarity.

Table 3. Comparison of Docking Studies Performed on **3** and **4**. Values Are the Root Mean Square Deviations (RMSDs) for All Non-H Atoms. For Direct Comparison, the Same Values for **1**, TSA, and SAHA Are Reported

compd	SAD or Exp vs DOCK	SAD or Exp vs Autodock	DOCK vs Autodock
3	3.2	3.1	1.4
4	2.2	2.8	1.5
1	5.6	3.8	5.1
TSA	1.0	1.4	1.9
SAHA	1.5	2.3	2.0

In all cases except for the Autodock internal scoring function predicted K_i value of **3**, binding affinities of **3** and **4** were predicted from 1.3- to 354.8- (**3**) and from 1.20- to 616.6-times (**4**) higher than those of **1** against HDAC1 (Table 1). From these encouraging data the synthesis of **3** and **4** has been performed, and their in vitro anti-HDAC (antimouse HDAC1 and antimaize HD2) activities have been assessed.

Chemistry. Vilsmeier−Haack reaction performed on 2-benzoyl-1-methyl-1*H*-pyrrole[38] afforded 2-benzoyl-1-methyl-1*H*-pyrrole-5-carboxaldehyde **5** and its corresponding 4-isomer **6**[39] in high yields. Pyrrolecarboxaldehydes **5**,**6** were treated with triethyl phosphonoacetate in the presence of potassium carbonate under Wittig−Horner conditions to afford the related ethyl pyrrole-5-propenoate **7** and -4-propenoate **8**, which were in turn converted into the corresponding pyrrolepropenoic acids **9** and **10** by alkaline hydrolysis. Finally, reaction of **9**,**10** with ethyl chloroformate and hydroxylamine furnished the desired hydroxamates **3**,**4** (Scheme 1).

Scheme 1[a]

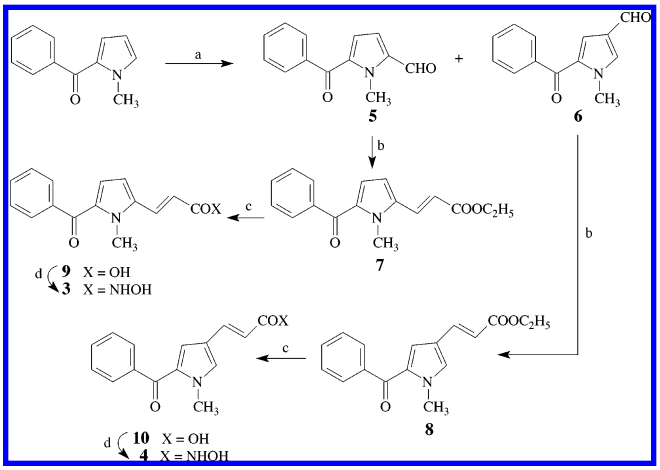

[a] Reagents and conditions: (a) $(COCl)_2$, DMF, dichloroethane, 0 °C; (b) $(C_2H_5O)_2OPCH_2COOC_2H_5$, K_2CO_3, C_2H_5OH, 80 °C; (c) KOH, C_2H_5OH, H_2O, 70 °C; (d) (1) $ClCOOC_2H_5$, $(C_2H_5)_3N$, THF, 0 °C; (2) NH_2OH, rt.

Table 4. Antimaize HD2 and Antimouse HDAC1 Activities of Compounds **3** and **4**[a]

	maize HD2		
compd	% inhbtn[b]	$IC_{50} \pm$ SD (μM)	mouse HDAC1, $IC_{50} \pm$ SD (μM)
3	95	0.28 ± 0.014	0.25 ± 0.01
4	97	0.05 ± 0.003	0.78 ± 0.04
1[27]	86	3.8 ± 0.1	4.9 ± 0.1
TSA[27]		0.0072 ± 0.0003	0.002 ± 0.00006
SAHA[27]		0.05 ± 0.002	0.112 ± 0.004

[a] Data represent mean values of at least three separate experiments. [b] Percent of inhibition at 30 μM.

Results and Discussion

Inspection of 3 and 4 Binding Modes. Comparison between Predicted and Experimental HDAC1 Inhibitory Activities. As the newly designed derivatives **3** and **4** were predicted by computational tools up to 617-fold more potent than **1** against HDAC1, they were synthesized and tested against both mouse HDAC1 and maize HD2 enzymes. Maize HD2, which was characterized in detail by us,[25,40−44] has an in vitro enzyme activity comparable to those of HDACs from other sources, such as fungi and vertebrates, using our standard HDAC assay.[40,44] Moreover, maize HD2 has shown a good mammalian deacetylase predictive value in various series of HDAC inhibitors.[25,27−29,45,46] TSA and SAHA were tested together with the pyrrole compounds as reference drugs.

The results, expressed as percent of enzyme inhibition at fixed dose and IC_{50} (50% inhibitory concentration) values, are reported in Table 4.

In anti-HD2 assay, **3** and **4** were 16- and 76-times more effective in inhibiting the enzyme than **1**, **4** being as potent as SAHA and 7-times less active than TSA. As anti-HDAC1 agents, **3** and **4** were less potent than

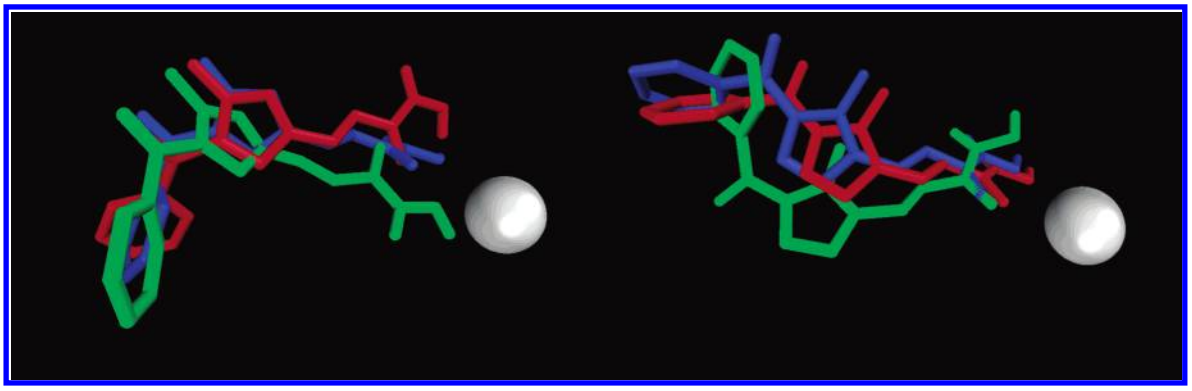

Figure 3. Superimposition of the docked conformations of APHA isomers **3** (right) and **4** (left) obtained from the three docking procedures (see text). The semiautomatic docked (SAD) conformations are in green. Autodock conformations are in red. DOCK conformations are in blue. The gray sphere indicate the Zn ion position into the HDAC1. The same 3D orientation is kept for direct comparison.

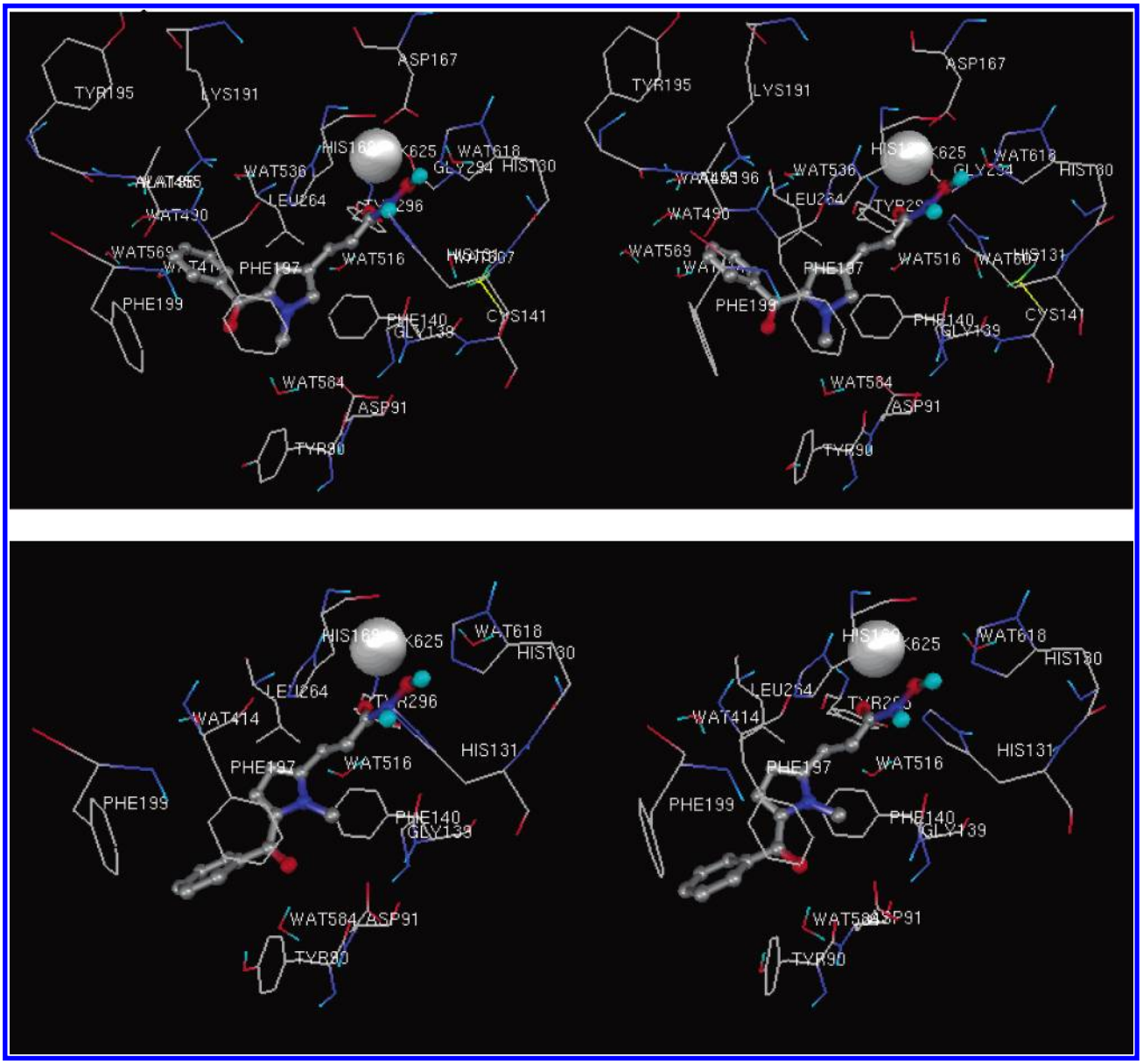

Figure 4. Autodock binding mode of APHA isomers **3** (bottom) and **4** (top). Inhibitors are drawn in ball-and-stick. For the sake of clarity, only a 3 Å core of the HDAC1 with essential hydrogen atoms is displayed. Residue numbering is reported for description without correction relative to the real HDAC1 sequence.

TSA and SAHA, but were 19- and 6-times more active than **1**, respectively.

K_i values of **3** and **4** were predicted by VALIDATE and Autodock means from 1.3- to 354.8- and from 1.20-

Table 5. Calculated Steric Fit Values[37] and Hydroxamate/Zn Distances of **1**, **3**, and **4**

compd	docking method	steric fit	CO···Zn	OH···Zn
1	SAD	1.3	4.5	4.8
	Autodock	2.3	2.8	4.4
	DOCK	1.5	4.7	4.8
3	SAD	1.46	3.7	2.2
	Autodock	1.94	2.8	3.0
	DOCK	1.94	3.3	3.0
4	SAD	1.85	2.9	3.0
	Autodock	1.85	2.8	3.5
	DOCK	1.85	2.9	3.0

to 616.6- times higher than those of **1** against HDAC1, respectively (Table 1). Such predictions of activity have been fully confirmed by experimental data.

By comparing the docking studies performed on **3** and **4**, it is possible to observe that docking studies highly agree each other, displaying clustered binding conformations for either isomer **3** or **4** (Figure 3).

These data agree with our previous findings[28] that low active compounds (i.e., isomer **1**) bind the deacetylase core in a lousy way and probably with a not fully defined binding conformation. On the other hand, in this study we found that the pyrrole ring rotation between benzoyl and *N*-hydroxy-2-propenamide moieties critically affects the binding mode of APHA isomers. In fact (Figure 3), while the *N*-hydroxy-2-propenamide tail maintains a similar conformation for either isomer **3** or **4**, the *N*-methylpyrrole and benzoyl moieties are clearly disposed in different ways (compare left side with right side of Figure 3). Autodock binding conformations of **3** (bottom) and **4** (top) are depicted in Figure 4. Either isomer **3** or **4** fits into the HDAC1 binding cavity considerably better then **1** (compare steric fit values in Table 5), thus providing a closer positioning of either **3** or **4** hydroxamate moiety to the zinc ion (**1**: average CO···Zn = 4.0 Å, average OH···Zn = 4.7 Å; **3**: average CO···Zn = 3.3 Å, average OH···Zn = 2.7 Å; **4**: average CO···Zn = 2.9 Å, average OH···Zn = 3.2 Å).

Inspection of the Autodock **3** and **4** binding modes clearly highlights the key role of the virtual pyrrole ring rotation. In the case of isomer **4** (top of Figure 4), the *N*-methylpyrrole group does not make crucial interactions with any HDAC1 residues, allowing the propenoylhydroxamate tail to fit into the Zn-containing well and to make the following favorable interactions: (i) positive π-stacking interactions between the pyrrolylethylene chain and Phe140 and Phe197 residues; (ii) hydrogen bond net between CONHOH moiety and the catalytic residues side chains (His130, His131, Asp167) plus the catalytic water (Wat618), and (iii) hydrogen bond between amidic carbonyl oxygen and Tyr296 hydroxyl group. In the case of isomer **3**, a slightly different scenario can be observed (bottom of Figure 4). While the CONHOH group and the pyrrolylethylene chain place the same interactions made by the corresponding portions of **4**, the *N*-methyl group of **3** makes favorable interactions with the C_α carbon atom of Gly139, and the benzoyl oxygen seems to be involved in a water-bridged hydrogen bond with Tyr90. These further interactions could account for the **3** slightly higher HDAC1 inhibitory activity than that observed for **4**, as also recorded by the VALIDATE prediction on the Autodock proposed complexes (**4**: $IC_{50-HDAC1}$ = 0.78 μM, VALIDATE predicted $K_{i\ HDAC1-Autodock}$ = 0.03 μM; **3**: $IC_{50-HDAC1}$ = 0.25 μM, VALIDATE predicted $K_{i\ HDAC1-Autodock}$ = 0.02 μM).

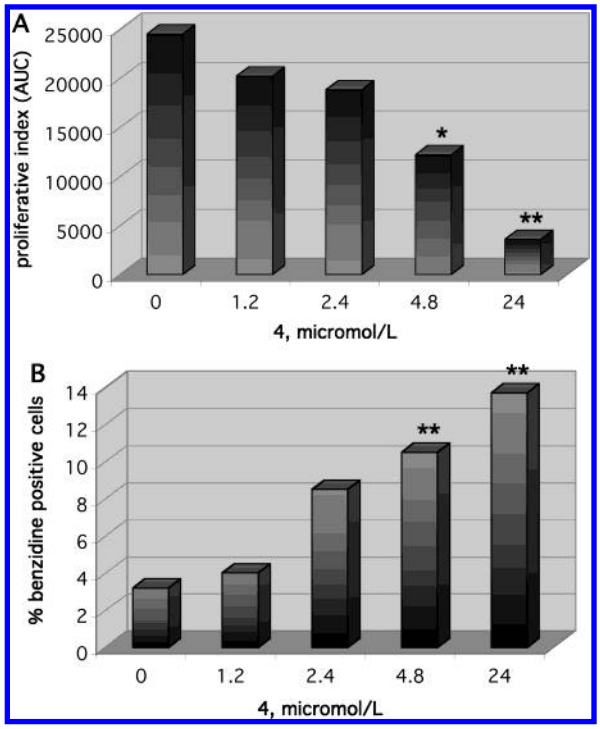

Figure 5. Antiproliferative and cytodifferentiating effects of **4** on MEL cell line. (A) Effects of **4** on cell growth of MEL cells, cultured for 48 h. Data are expressed as area under the curve (AUC) (mean ± SEM, $n = 4$); *, $p < 0.05$; **, $p < 0.01$. (B) Effects of **4** on differentiation of MEL cells. The cells were cultured with various concentrations of drug for 48 h. Each point is the mean ± SEM ($n = 4$); **, $p < 0.01$.

Antiproliferative and Cytodifferentiating Effects of 4 on Friend Murine Erythroleukemia (MEL) Cells. In addition to in vitro enzyme assays, the capability of **4** to induce antiproliferative and cytodifferentiating effects in vivo on Friend MEL cells were evaluated. Figure 5A shows the effect of **4** on the growth of MEL cells, cultured for 48 h. Such compounds showed significant dose-dependent inhibitory effect on the growth rate of cell line ($p < 0.01$). Moreover, after 48 h the inhibitor was not cytotoxic at the tested concentrations (data not shown).

In MEL cells, benzidine staining reveals the hemoglobin accumulation rate, which is related to the activation of the cell line differentiation process. The results (Figure 5B) clearly indicate a dose-dependent increase of hemoglobin synthesis for **4** at the tested doses.

Conclusion

Aroyl-pyrrole-hydroxy-alkylamides (APHAs) are a new class of synthetic HDAC inhibitors recently described by us.[25,27−29] Through three different docking procedures, we designed, synthesized, and tested two new APHA isomers, compounds **3** and **4**, characterized by different insertions of benzoyl and propenoylhydroxamate groups onto the pyrrole ring. As biological activities of **3** and **4** were predicted by computational tools up to 617-fold more potent than that of lead compound **1** against HDAC1, **3** and **4** were synthesized and tested against both mouse HDAC1 and maize HD2 enzymes. Predictions of biological affinities (K_i values) of **3** and **4**, performed by a VALIDATE model (applied on either

SAD or automatic DOCK or Autodock results) and by the Autodock internal scoring function, were in good agreement with experimental activities. Clearly, in comparison with the **1** structure, the switching of *N*-methylpyrrole ring introduced some conformational changes in the APHA binding mode leading to further ligand/receptor positive interactions and higher HDAC1 inhibitory activities. Particularly, in mouse HDAC1 inhibitory assay **3** and **4** were 19- and 6-times more active than **1**, respectively. Against maize HD2, **3** and **4** were 16- and 76-times more effective in inhibiting the enzyme than **1**, **4** being as potent as SAHA in this assay.

Compound **4**, tested as antiproliferative and cytodifferentiating agent on MEL cells, showed dose-dependent growth inhibition, significant at 4.8 ($p < 0.05$) and 24 ($p < 0.01$) μM, and dose-dependent hemoglobin accumulation effect, highly significant ($p < 0.01$) at 4.8 μM.

In conclusion, the two APHA isomers **3** and **4** can be considered as new lead compounds in the anti-HDAC field. We are currently investigating the effect of chemical modifications at both benzoyl moieties and *N*-hydroxy-2-propenamide chains of **3** and **4** on the enzyme inhibitory activity.

Experimental Section

Chemistry. Melting points were determined on a Büchi 530 melting point apparatus and are uncorrected. Infrared (IR) spectra (KBr) were recorded on a Perkin-Elmer Spectrum One instrument. ^{1}H NMR spectra were recorded at 200 MHz on a Bruker AC 200 spectrometer; chemical shifts are reported in δ (ppm) units relative to the internal reference tetramethylsilane (Me_4Si). All compounds were routinely checked by TLC and ^{1}H NMR. TLC was performed on aluminum-backed silica gel plates (Merck DC−Alufolien Kieselgel 60 F_{254}) with spots visualized by UV light. All solvents were reagent grade and, when necessary, were purified and dried by standards methods. Concentration of solutions after reactions and extractions involved the use of a rotary evaporator operating at a reduced pressure of ca. 20 Torr. Organic solutions were dried over anhydrous sodium sulfate. Analytical results are within ±0.40% of the theoretical values. A SAHA sample for biological assays was prepared as previously reported by us.[47] All chemicals were purchased from Aldrich Chimica, Milan (Italy) or Lancaster Synthesis GmbH, Milan (Italy) and were of the highest purity.

2-Benzoyl-1-methyl-1*H*-pyrrole-5-carboxaldehyde (5) and 2-Benzoyl-1-methyl-1*H*-pyrrole-4-carboxaldehyde (6). A 50 mL 1,2-dichloroethane solution of oxalyl chloride (0.06 mol, 5.2 mL) was added to a cooled (0−5 °C) solution of *N*,*N*-dimethylformamide (0.06 mol, 4.6 mL) in 1,2-dichloroethane (50 mL) over a period of 5−10 min. After being stirred at room temperature for 15 min, the suspension was cooled (0−5 °C) again and treated with a solution of 2-benzoyl-1-methyl-1*H*-pyrrole[38] (0.06 mol, 11.1 g) in 1,2-dichloroethane (50 mL). The mixture was stirred at room temperature for 1 h and then was poured onto crushed ice (200 g) containing 50% NaOH (50 mL) and stirred for 10 min. The pH of the solution was adjusted to 4 with 37% HCl, the organic layer was separated, and the aqueous one was extracted with chloroform (2 × 50 mL). The combined organic solutions were washed with water, dried, and evaporated to dryness. The residual oil was chromatographed on silica gel eluting with ethyl acetate:chloroform 1:10. The first eluates were collected and evaporated to afford **5** as a pure solid; further elution gave **6**[39] as a pure solid.

5: yield: 44%; mp: 90−91 °C, recrystallization solvent: cyclohexane; ^{1}H NMR ($CDCl_3$) δ 4.23 (s, 3 H, CH_3), 6.62 (m, 1 H, pyrrole β-proton), 6.87 (m, 1 H, pyrrole β-proton), 7.44 (m, 3 H, benzene H-3,4,5), 7.78 (m, 2 H, benzene H-2,6), 9.77 (s, 1 H, CHO). Anal. ($C_{13}H_{11}NO_2$) C, H, N.

6:[39] yield: 56%; mp: 108−109 °C, recrystallization solvent: cyclohexane; ^{1}H NMR ($CDCl_3$) δ 4.04 (s, 3 H, CH_3), 7.12 (d, 1 H, pyrrole β-proton), 7.47 (m, 4 H, pyrrole α-proton and benzene H-3,4,5), 7.76 (m, 2 H, benzene H-2,6), 9.74 (s, 1 H, CHO). Anal. ($C_{13}H_{11}NO_2$) C, H, N.

General Procedure for the Synthesis of Ethyl 3-(2-Benzoyl-1-methyl-1*H*-pyrrol-5- and -4-yl)propenoates 7,8. Example: Ethyl 3-(2-Benzoyl-1-methyl-1*H*-pyrrol-5-yl)-propenoate (7). A suspension of **5** (6.0 mmol, 1.28 g) in absolute ethanol (20 mL) was added in one portion to a mixture of triethyl phosphonoacetate (7.2 mmol, 1.5 mL) and anhydrous potassium carbonate (18.0 mmol, 2.5 g). After being stirred at 70 °C for 2 h, the reaction mixture was cooled to room temperature, diluted with water (50 mL), and extracted with ethyl acetate (3 × 30 mL). The organic layer was washed with water, dried, and evaporated to dryness, and the solid residue was recrystallized to furnish pure **7**.

7: yield: 65%; mp: 88−89 °C, recrystallization solvent: cyclohexane; ^{1}H NMR ($CDCl_3$) δ 1.30 (t, 3 H, CH_2CH_3), 4.03 (s, 3 H, NCH_3), 4.23 (q, 2 H, CH_2CH_3), 6.35 (d, 1 H, CH=CHCO), 6.56 (d, 1 H, pyrrole β-proton), 6.65 (d, 1 H, pyrrole β-proton), 7.45 (m, 4 H, CH=CHCO and benzene H-3,4,5), 7.73 (m, 2 H, benzene H-2,6). Anal. ($C_{17}H_{17}NO_3$) C, H, N.

8: yield: 62%; mp: 83−84 °C, recrystallization solvent: cyclohexane/benzene; ^{1}H NMR ($CDCl_3$) δ 1.26 (t, 3 H, CH_2CH_3), 3.98 (s, 3 H, NCH_3), 4.18 (q, 2 H, CH_2CH_3), 6.08 (d, 1 H, CH=CHCO), 6.85 (d, 1 H, pyrrole β-proton), 7.08 (d, 1 H, pyrrole α-proton), 7.46 (m, 4 H, CH=CHCO and benzene H-3,4,5), 7.74 (m, 2 H, benzene H-2,6). Anal. ($C_{17}H_{17}NO_3$) C, H, N.

General Procedure for the Synthesis of 3-(2-Benzoyl-1-methyl-1*H*-pyrrol-5- and -4-yl)propenoic Acids 9,10. Example. 3-(2-Benzoyl-1-methyl-1*H*-pyrrol-4-yl)propenoic Acid (10). A mixture of **8** (5.7 mmol, 1.61 g), 2 N KOH (22.9 mmol, 11.4 mL), and ethanol (15 mL) was heated at 70 °C for 3 h. After cooling, the solution was poured into water (50 mL) and extracted with ethyl acetate (2 × 20 mL). To the aqueous layer was added 2 N HCl until the pH was 5, and the precipitate was filtered and recrystallized from benzene giving the pure compound **10**.

9: yield: 75%; mp: 222−223 °C, recrystallization solvent: benzene; ^{1}H NMR (DMSO-d_6) δ 3.93 (s, 3 H, NCH_3), 6.46 (d, 1 H, CH=CHCO), 6.59 (d, 1 H, pyrrole β-proton), 6.83 (d, 1 H, pyrrole β-proton), 7.53 (m, 4 H, CH=CHCO and benzene H-3,4,5), 7.66 (m, 2 H, benzene H-2,6), 12.40 (s, 1 H, OH). Anal. ($C_{15}H_{13}NO_3$) C, H, N.

10: yield: 69%; mp: 209−210 °C, recrystallization solvent: benzene; ^{1}H NMR (DMSO-d_6) δ 3.87 (s, 3 H, NCH_3), 6.12 (d, 1 H, CH=CHCO), 6.97 (d, 1 H, pyrrole β-proton), 7.54 (m, 4 H, CH=CHCO and benzene H-3,4,5), 7.70 (m, 3 H, pyrrole α-proton and benzene H-2,6). Anal. ($C_{15}H_{13}NO_3$) C, H, N.

General Procedure for the Synthesis of 3-(2-Benzoyl-1-methyl-1*H*-pyrrol-5- and -4-yl)-*N*-hydroxypropenamides 3,4. Example. 3-(2-Benzoyl-1-methyl-1*H*-pyrrol-4-yl)-*N*-hydroxypropenamide (4). Ethyl chloroformate (5.0 mmol, 0.5 mL) and triethylamine (5.4 mmol, 0.8 mL) were added to a cooled (0 °C) solution of **10** (4.2 mmol, 1.07 g) in dry THF (10 mL), and the mixture was stirred for 10 min. The solid was filtered off. The filtrate was added to a freshly prepared solution of hydroxylamine, obtained by reaction between hydroxylamine hydrochloride (6.2 mmol, 0.4 g) and KOH (6.2 mmol, 0.35 g) in methanol (10 mL). After being stirred at room temperature for 15 min, the mixture was evaporated under reduced pressure and the residue was recrystallized from benzene to give the pure compound **4**.

3: yield: 42%; mp: 134−136 °C, recrystallization solvent: benzene; ^{1}H NMR (DMSO-d_6) δ 3.93 (s, 3 H, NCH_3), 6.42 (d, 1 H, CH=CHCO), 6.58 (d, 1 H, pyrrole β-proton), 6.80 (d, 1 H, pyrrole β-proton), 7.40 (d, 1 H, CH=CHCO), 7.54 (m, 3 H, benzene H-3,4,5), 7.67 (m, 2 H, benzene H-2,6), 9.00 (s, 1 H, NH), 10.36 (s, 1 H, OH). Anal. ($C_{15}H_{14}N_2O_3$) C, H, N.

4: yield: 54%; mp: 144−145 °C, recrystallization solvent: benzene; ^{1}H NMR (DMSO-d_6) δ 3.88 (s, 3 H, NCH_3), 6.04 (d, 1 H, CH=CHCO), 6.76 (s, 1 H, pyrrole β-proton), 7.24 (d, 1 H, CH=CHCO), 7.54 (m, 4 H, pyrrole α-proton and benzene H-3,4,5), 7.70 (m, 2 H, benzene H-2,6), 8.80 (s, 1 H, NH), 10.40 (s, 1 H, OH). Anal. ($C_{15}H_{14}N_2O_3$) C, H, N.

Molecular Modeling Studies. All molecular modeling calculations and manipulations were performed using the software packages Macromodel 7.1,[32] MOPAC 2000,[35,36] VALIDATE,[37] GOLPE 4.5.12,[48] XlogP 2,[49] Autodock 3.0.5,[31] DOCK 4.0.2,[30] and MIDAS 2.1[50] running on Silicon Graphics O2 R10000, IBM-compatible AMD Athlon 2.4 GHz workstations. For the conformational analysis and for any minimization the all-atom Amber force field[33,34] was adopted as implemented in the Macromodel package. As previously reported[26] the crystal structure of TSA extracted from the HDLP/TSA complex filed in the Brookhaven Protein Data Bank[51] (entry code 1c3r) was used. The HDAC1 model was constructed from HDLP as previously reported.[27] Before any docking studies the HDAC1 model was minimized in a vacuum in the presence of TSA to relieve any steric contact introduced by the mutated residue's side chains.

Simulated annealing (SA) run were also performed either in water or in a vacuum on the HDAC1 model with and without the bound TSA. Comparison of the roughly minimized HDAC1/TSA complex with the results of the SA dynamic runs showed very low RMSD values on the C_α traces, also including the residue side-chains, thus revealing that the direct use of the minimized virtual HDAC1 is a fast and reliable choice.

Binding modes of **3** and **4** were extensively analyzed by the mean of three different docking procedures. A semiautomatic docking (SAD) was conducted similarly to that reported for **1**. A family of more than 200 conformations for either **3** and **4** was generated using the following procedure: the initial conformation of **3** or **4** obtained from the reported bound conformation of **1** was arbitrarily rotated by a step of 10° along an axis passing through the center of the benzene ring and the hydroxamic acid carbon atom. Each of the obtained new 36 HDAC1/**3** or HDAC1/**4** complexes was submitted to a grid search rotating the five dihedral angles by a step of 30°. By filtering out all of the complexes showing a molecular clashing between **3** or **4** and the enzyme pocket, the final conformation families were achieved. After minimization, the chosen binding conformations of **3** and **4** were those associated with the most stable complexes (global minimum).

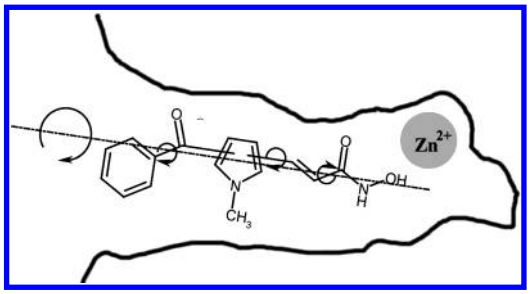

The **3** and **4** starting conformations for the docking studies were obtained using molecular dynamics with simulated annealing as implemented in Macromodel version 7.1 and conducted as following: the molecules were energy minimized to a low gradient. The nonbonded cutoff distances were set to 20 Å for both van der Waals and electrostatic interactions. An initial random velocity to all atoms corresponding to 300 K was applied. Three subsequent molecular dynamics runs were then performed. The first was carried out for 10 ps with a 1.5 fs time-step at a constant temperature of 300 K for equilibration purposes. The next molecular dynamic was carried out for 20 ps, during which the system is coupled to a 150 °C thermal bath with a time constant of 5 ps. The time constant represents approximately the half-life for equilibration with the bath; consequently, the second molecular dynamic command caused the molecule to slowly cool to approximately 150 K. The third and last dynamic cooled the molecule to 50 K over 20 ps. A final energy minimization was then carried out for 250 iterations using conjugate gradient. The minimizations and the molecular dynamics were in all cases performed in aqueous solution. The atom charges automatically assigned by the batchmin module were retained on **3** or **4** for the docking calculations.

For the second docking procedure the program Autodock was used to explore the binding conformation of either **3** or **4**. For the docking a grid spacing of 0.375 Å and 58 × 52 × 48 number of points were used. The grid was centered on the mass center of the experimental bound TSA coordinates. The GA-LS method was adopted using the default settings. Amber united atoms were assigned to the protein using the program ADT (Auto Dock Tools). Autodock generated 100 possible binding conformations for **3** and **4**.

The third docking was performed by the mean of the program DOCK. First, a Connolly surface of each receptor active site was generated by using a 1.4 Å probe radius and further used to generate a set of overlapping spheres that were then clustered according to their spatial distribution. To optimize docking accuracy, spheres located too far away from the known ligand position were eliminated from the finally selected cluster. To compute interaction energies, a 3-D grid of 0.30 Å resolution was centered on TSA experimental bound conformation. The size of the grid box was chosen to enclose all selected spheres using an extra margin of 6 Å. The grid had a size of about 36 × 31 × 33 Å and comprised about 1400000 grid points. Energy scoring grids were obtained by using an all-atom model and a distance-dependent dielectric function ($\epsilon = 4r$) with a 10 Å cutoff. Amber atomic charges were assigned to all protein atoms. The ligands were then docked in turn into the protein active site by matching sphere centers with ligand atoms. A flexible docking (peripheral search and torsion drive) with subsequent minimization was performed as follows: (i) automatic selection and matching of an anchor fragment within a maximum of 10000 orientations, (ii) iterative growing of the ligand using at least 30 conformations (peripheral seeds) for seeding the next growing stage with assignment of energy-favored torsion angles, (iii) simultaneous relaxation of the base fragments as well as of all peripheral segments and final relaxation of the entire molecule. Orientations/conformations were relaxed in 100 cycles of 100 simplex minimization steps to a convergence of 0.1 kcal/mol. The top 50 solutions corresponding to the best Dock energy scores were then stored in a single multi mol2 file.

Because of neither Autodock nor DOCK are able to perform any energy minimization of the generated complexes, the selection of the binding conformation for **3** or **4** was not straightforward by using the first Autodock/DOCK scored conformation. The selection of the binding conformation was performed by an energy based rescoring of the Autodock cluster representants and the 50 best contact scored DOCK conformations. The Macromodel program was used to minimize the corresponding 32 Autodock and the 50 DOCK HDAC1/**3** or HDAC1/**4** complexes. The ligand and an 10 Å core of atoms of the pocket were let to relax during the minimization. An external fixed shell of 8 Å was also included for the long-range interactions. Because of the presence of a metal Zn ion in the HDAC1 catalytic core and the intrinsic molecular mechanic electrostatic limitation of the AMBER force field the minimizations were performed applying AM1 charges calculated with the program MOPAC 2000.

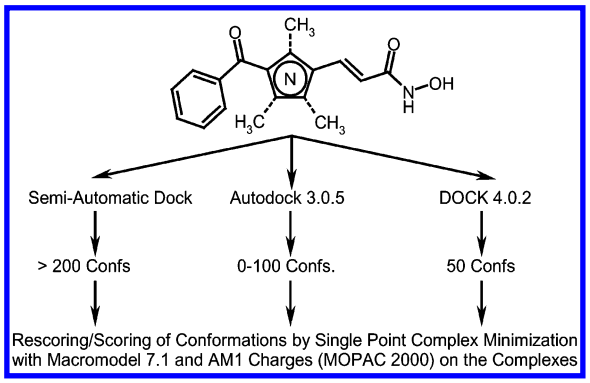

The VALIDATE procedure was used to estimate the binding conformation of the docking studies as previously reported. The partition coefficients were calculated using the program XlogP.

Biological Assays. HD2 Enzyme Inhibition. Radioactively labeled chicken core histones were used as the enzyme substrate according to established procedures.[40] The enzyme liberated tritiated acetic acid from the substrate which was quantitated by scintillation counting. IC_{50} values are results of triple determinations. Maize enzyme (50 μL) (at 30 °C) was incubated (30 min) with 10 μL of total [^{3}H]acetate-prelabeled chicken reticulocyte histones (4 mg/mL). Reaction was stopped by addition of 36 μL of 1 M HCl/0.4 M acetate and 800 μL of ethyl acetate. After centrifugation (10 000*g*, 5 min), an aliquot of 600 μL of the upper phase was counted for radioactivity in 3 mL of liquid scintillation cocktail. The compounds were tested in a starting concentration of 40 μM, and active substances were diluted further. Sodium butyrate, sodium valproate, TSA, SAHA,[47] trapoxin, and HC-toxin were used as the reference compounds, and blank solvents were used as negative controls.

Mouse HDAC1 Enzyme Assay. For inhibition assay, partially purified HDAC1 from mouse A20 cells (ATCC: TIB-208) (anion exchange chromatography, affinity chromatography was used as enzyme source. HDAC activity was determined as described[52] using [^{3}H]acetate-prelabeled chicken reticulocyte histones as substrate. 50 μL of mouse HDAC1 were incubated with different concentrations of compounds for 15 min on ice and 10 μL of total [^{3}H]acetate-prelabeled chicken reticulocyte histones (4 mg/mL) were added, resulting in a concentration of 41 μM. The mixture was incubated at 37 °C for 1 h. The reaction was stopped by addition of 50 μL of 1 M HCl/0.4 M acetylacetate and 1 mL ethyl acetate. After centrifugation at 10 000*g* for 5 min an aliquot of 600 μL of the upper phase was counted for radioactivity in 3 mL of liquid scintillation cocktail.

Growth Inhibition and Cell Differentiation Assay. Cell Culture and Reagents. Murine erythroleukemia (MEL) cells were obtained from Interlab Cell Line Collection (CBA) (Genoa, Italy). Cells were maintained at 37 °C under a humidified atmosphere of 5% CO_2 in RPMI 1640 Hepes modified medium supplemented with 10% (v/v) heat inactivated foetal calf serum, 2 mmol/L glutamine, 100 IU/mL penicillin and 100 μg/mL streptomycin. Unless indicated all chemicals and reagents (cell culture grade) were obtained from Sigma Chemical Co., Milan, Italy.

Cell Viability and Growth Inhibition Assay. Cell number was determined using a Neubauer hemocytometer, and viability was assessed by their ability to exclude trypan blue.

The stock solutions were prepared immediately before use. Compound **4** was dissolved in DMSO. MEL exponentially growing cells (1×10^5 cells/mL) were set at day 0 in media containing various concentrations of drugs for 48 h. The final concentrations of the drug were: 1.2, 2.4, 4.8, and 24 μM. The final concentration of DMSO, used as vehicle, was the same (0.1% v/v) in all samples during the experiments.

Cytomorphological Assay for MEL Cell Differentiation. The most widely used method for scoring erythroid differentiation is benzidine staining which reveals the production of hemoglobin.[53] Benzidine dihydrochloride (2 mg/mL) was prepared in 3% acetic acid. Hydrogen peroxide (1%) was added immediately before use. The MEL cell suspensions were mixed with the benzidine solution in a 1:1 ratio and counted in a hemocytometer after 5 min. Blue cells were considered to be positive for hemoglobin.

Statistical Analysis. All results are expressed as mean ± SEM. The group means were compared by analysis of variance (ANOVA) followed by a multiple comparison of means by Dunnet test; $p < 0.05$ was considered significant.

Acknowledgment. This work was supported by grants of "Progetto Finalizzato Ministero della Salute 2002" (A.M.), "AIRC Proposal 2003" (A.M.), and the Austrian Science Foundation P13209 (G.B.) and P13620 (P.L.).

References

(1) Wu, J.; Grunstein, M. 25 Years after the nucleosome model: chromatin modifications. *Trends Biochem. Sci.* **2000**, *25*, 619−623.
(2) Urnov, F. D.; Wolffe, A. Chromatin organization and human disease. *Emerg. Ther. Targets* **2000**, *4*, 665−685.
(3) Pazin, M. J.; Kadonaga, J. T. What is up and down with histone deacetylation and transcription? *Cell* **1997**, *89*, 325−328.
(4) Grunstein, M. Histone acetylation in chromatin structure and transcription. *Nature* **1997**, *389*, 349−352.
(5) Davie, J. R. Covalent modifications of histones: expression from chromatin templates. *Curr. Opin. Genet. Dev.* **1998**, *8*, 173−178.
(6) Kouzarides, T. Histone acetylases and deacetylases in cell proliferation. *Curr. Opin. Genet. Dev.* **1999**, *9*, 40−48.
(7) Yoshida, M.; Kijima, M.; Akita, M.; Beppu, T. Potent and Specific Inhibition of Mammalian Histone Deacetylase both In Vivo and In Vitro by Trichostatin A. *J. Biol. Chem.* **1990**, *265*, 17174−17179.
(8) Kijima, M.; Yoshida, M.; Suguta, K.; Horinouchi, S.; Beppu, T. Trapoxin, an Antitumor Cyclic Tetrapeptide, Is an Irreversible Inhibitor of Mammalian Histone Deacetylase. *J. Biol. Chem.* **1993**, *268*, 22429−22435.
(9) Shute, R. E.; Dunlap, B.; Rich, D. H. Analogues of the Cytostatic and Antimitogenic Agents Chlamydocin and HC-Toxin: Synthesis and Biological Activity of Chloromethyl Ketone and Diazomethyl Ketone Functionalized Cyclic Tetrapeptides. *J. Med. Chem.* **1987**, *30*, 71−78.
(10) Han, J. W.; Ahn, S. H.; Park, S. H.; Wang, S. Y.; Bae, G. U.; Seo, D. W.; Known, H. K.; Hong, S.; Lee, Y. W.; Lee, H. W. Apicidin, a histone deacetylase inhibitor, inhibits proliferation of tumor cells via induction of p21WAF1/Cip1 and gelsolin. *Cancer Res.* **2000**, 60, 6068−6074.
(11) Richon, V. M.; Emiliani, S.; Verdin, E.; Webb, Y.; Breslow, R.; Rifkind, R. A.; Marks, P. A. A class of hybrid polar inducers of transformed cell differentiation inhibits histone deacetylases. *Proc. Natl. Acad. Sci. U.S.A.* **1998**, *95*, 3003−3007.
(12) Furumai, R.; Komatsu, Y.; Nishino, N.; Khochbin, S.; Yoshida, M.; Horinouchi, S. Potent histone deacetylase inhibitors built from trichostatin A and cyclic tetrapeptide antibiotics including trapoxin. *Proc. Natl. Acad. Sci. U.S.A.* **2001**, *98*, 87−92.
(13) Komatsu, Y.; Tomizaki, K.; Tsukamoto, M.; Kato, T.; Nishino, N.; Sato, S.; Yamori, T.; Tsuruo, T.; Furumai, R.; Yoshida, M.; Horinouchi, S.; Hayashi, H. Cyclic Hydroxamic-acid-containing Peptide 31, a Potent Synthetic Histone Deacetylase Inhibitor with Antitumor Activity. *Cancer Res.* **2001**, *61*, 4459−4466.
(14) Ueda, H.; Nakajima, H.; Hori, Y.; Fujita, T.; Nishimura, M.; Goto, T.; Okuhara, M. FR901228, a novel antitumor bicyclic depsipeptide produced by Chromobacterium violaceum No. 968. I. Taxonomy, fermentation, isolation, physicochemical and biological properties, and antitumor activity. *J. Antibiot.* **1994**, *47*, 301−310.
(15) Suzuki, T.; Ando, T.; Tsuchiya K.; Fukazawa, N.; Saito, A.; Mariko, Y.; Yamashita, T.; Nakanishi, O. Synthesis and Histone Deacetylase Inhibitory Activity of New Benzamide Derivatives. *J. Med. Chem.* **1999**, *42*, 3001−3003.
(16) Saito, A.; Yamashita, T.; Mariko, Y.; Nosaka, Y.; Tsuchiya, K.; Ando, T.; Suzuki, T.; Tsuruo, T.; Nakanishi, O. A synthetic inhibitor of histone deacetylase, MS-27−275, with marked in vivo antitumor activity against human tumors. *Proc. Natl. Acad. Sci. U.S.A.* **1999**, *96*, 4592−4597.
(17) Göttlicher, M.; Minucci, S.; Zhu, P.; Kramer, O. H.; Schimpf, A.; Giavara, S.; Sleeman, J. P.; Lo Coco, F.; Nervi, C.; Pelicci, P. G.; Heinzel, T. Valproic acid defines a novel class of HDAC inhibitors inducing differentiation of transformed cells. *EMBO J.* **2001**, *20*, 6969−6978.
(18) Phiel, C. J.; Zhang, F.; Huang, E. Y.; Guenther, M. G.; Lazar, M. A.; Klein, P. S. Histone deacetylase is a direct target of valproic acid, a potent anticonvulsant, mood stabilizer, and teratogen. *J. Biol. Chem.* **2001**, *76*, 36734−36741.
(19) Johnstone, R. W. Histone-deacetylase inhibitors: novel drugs for the treatment of cancer. *Nature Rev. Drug Discov*ery **2002**, *1*, 287−299.
(20) Vigushin, D. M.; Coombes, R. C. Histone deacetylase inhibitors in cancer treatment. *Anticancer Drugs* **2002**, *13*, 1−13.
(21) Kelly, W. K.; O'Connor, O. A.; Marks, P. A. Histone deacetylase inhibitors: from target to clinical trials. *Expert Opin. Investig. Drugs* **2002**, *11*, 1695−1713.
(22) Finnin, M. S.; Donigian, J. R.; Cohen, A.; Richon, V. M.; Rifkind, R. A.; Marks, P. A.; Breslow, R.; Pavletich, N. P. Structures of a histone deacetylase homologue bound to the TSA and SAHA inhibitors. *Nature* **1999**, *401*, 188−193.

(23) Massa, S.; Artico, M.; Corelli, F.; Mai, A.; Di Santo, R.; Cortes, S.; Marongiu, M. E.; Pani, A.; La Colla, P. Synthesis and Antimicrobial and Cytotoxic Activities of Pyrrole-Containing Analogues of Trichostatin A. *J. Med. Chem.* **1990**, *33*, 2845−2849.
(24) Corelli, F.; Massa, S.; Stefancich, G.; Mai, A.; Artico, M.; Panico, S.; Simonetti, N. Ricerche su composti antibatterici ed antifungini. Nota VIII − Sintesi ed attività antifungina di derivati pirrolici correlati con la tricostatina A. (Researches on antibacterial and antifungal agents. VIII. Synthesis and antifungal activity of trichostatin A-related pyrrole derivatives.) *Farmaco, Ed. Sci.* **1987**, *42*, 893−903.
(25) Massa, S.; Mai, A.; Sbardella, G.; Esposito, M.; Ragno, R.; Loidl, P.; Brosch, G. 3-(4-Aroyl-1*H*-pyrrol-2-yl)-*N*-hydroxy-2-propenamides, a New Class of Synthetic Histone Deacetylase Inhibitors. *J. Med. Chem.* **2001**, *44*, 2069−2072.
(26) Lusser, A.; Brosch, G.; Loidl, A.; Haas, H.; Loidl, P. Identification of maize histone deacetylase HD2 as an acidic nucleolar phosphoprotein. *Science* **1997**, *277*, 88−91.
(27) Mai, A.; Massa, S.; Ragno, R.; Esposito, M.; Sbardella, G.; Nocca, G.; Scatena, R.; Jesacher, F.; Loidl, P.; Brosch, G. Binding Mode Analysis of 3-(4-Benzoyl-1-methyl-1*H*-2-pyrrolyl)-*N*-hydroxy-2-propenamide: A New Synthetic Histone Deacetylase Inhibitor Inducing Histone Hyperacetylation, Growth Inhibition, and Terminal Cell Differentiation. *J. Med. Chem.* **2002**, *45*, 1778−1784.
(28) Mai, A.; Massa, S.; Ragno, R.; Cerbara, I.; Jesacher, F.; Loidl, P.; Brosch, G. 3-(4-Aroyl-1-methyl-1*H*-2-pyrrolyl)-*N*-hydroxy-2-alkylamides as a New Class of Synthetic Histone Deacetylase Inhibitors. 1. Design, Synthesis, Biological Evaluation, and Binding Mode Studies Performed Through Three Different Docking Procedures. *J. Med. Chem.* **2003**, *46*, 512−524.
(29) Mai, A.; Massa, S.; Cerbara, I.; Valente, S.; Ragno, R.; Bottoni, P.; Scatena, R.; Loidl, P.; Brosch, G. 3-(4-Aroyl-1-methyl-1*H*-2-pyrrolyl)-*N*-hydroxy-2-propenamides as a New Class of Synthetic Histone Deacetylase Inhibitors. 2. Effect of Pyrrole C2 and/or C4 Substitutions on Biological Activity. *J. Med. Chem.*, in press.
(30) Oshiro, C. M.; Kuntz, I. D.; Dixon, J. S. Flexible ligand docking using a genetic algorithm. *J. Comput. Aided Mol. Des.* **1995**, *9*, 113−130.
(31) Goodsell, D. S.; Morris, G. M.; Olson, A. J. Automated docking of flexible ligands: applications of AutoDock. *J. Mol Recognit.* **1996**, *9*, 1−5.
(32) Mohamadi, F.; Richards, N. G. J.; Guida, W. C.; Liskamp, R.; Lipton, M.; Caufield, C.; Chang, G.; Hendrickson, T.; Still, W. C. MACROMODEL − an integrated software system for modeling organic and bioorganic molecules using molecular mechanics. *J. Comput. Chem.* **1990**, *11*, 440−467.
(33) Pearlman, D. A.; Case, D. A.; Caldwell, J. W.; Ross, W. S.; Cheatham T. E., III; Debolt, S.; Ferguson, D. M.; Seibel, G. L.; Kollman, P. A. AMBER, a Package of Computer Programs for Applying Molecular Mechanics, Normal-Mode Analysis, Molecular Dynamics and Free Energy Calculations to Simulate the Structural and Energetic Properties of Molecules. *Comput. Phys. Commun.* **1995**, *91*, 1−41.
(34) Pearlman, D. A.; Case, D. A.; Caldwell, J. W.; Ross, W. S.; Cheatham, T. E.; III, Ferguson, D. M.; Seibel, G. L.; Singh, U. C.; Weiner, P. K.; Kollman, P. A. AMBER 4.1; Department of Pharmaceutical Chemistry, University of California: San Francisco, CA, 1995.
(35) Stewart, J. J. MOPAC: a semiempirical molecular orbital program. *J. Comput. Aided Mol. Des.* **1990**, *4*, 1−105.
(36) *MOPAC 2000.00 Manual*; Stewart, J. J. P., Ed; Fujitsu Limited: Tokyo, Japan (1999).
(37) Head, R. D.; Smythe, M. L.; Oprea, T. I.; Waller, C. L.; Green, S. M.; Marshall, G. R. VALIDATE: A New Method for the Receptor-Based Prediction of Binding Affinities of Novel Ligands. *J. Am. Chem. Soc.* **1996**, *118*, 3959−3969.
(38) Brittain, J. M.; Jones, R. A.; Arques, J. S.; Saliente, T. A. Pyrrole studies. XXVII. Utilization of 1-methyl-2-pyrrolyllithium in the synthesis of 1-methyl-2-substituted pyrroles. *Synth. Commun.* **1982**, *12*, 231−248.
(39) Lehr, M. Structure−Activity Relationships of (4-Acylpyrrol-2-yl)alkanoic Acids as Inhibitors of the Cytosolic Phospholipase A_2: Variation of the Substituent in Positions 1, 3, and 5. *J. Med. Chem.* **1997**, *40*, 3381−3392.
(40) Lechner, T.; Lusser, A.; Brosch, G.; Eberharter, A.; Goralik-Schramel, M.; Loidl, P. A comparative study of histone deacetylases of plant, fungal and vertebrate cells. *Biochim. Biophys. Acta* **1996**, *1296*, 181−188.
(41) Brosch, G.; Lusser, A.; Goralik-Schramel, M.; Loidl, P. Purification and characterization of a high molecular weight histone deacetylase complex (HD2) of maize embryos. *Biochemistry* **1996**, *35*, 15907−15914.
(42) Kölle, D.; Brosch, G.; Lechner, T.; Lusser, A.; Loidl, P. Biochemical methods for analysis of histone deacetylases. *Methods* **1998**, *15*, 323−331.
(43) Kölle, D.; Brosch, G.; Lechner, T.; Pipal, A.; Helliger, W.; Taplick, J.; Loidl, P. Different types of maize histone deacetylases are distinguished by a highly complex substrate and site specificity. *Biochemistry* **1999**, *38*, 6769−6773.
(44) Brosch, G.; Ransom, R.; Lechner, T.; Walton, J.; Loidl, P. Inhibition of maize histone deacetylases by HC toxin, the host-selective toxin of Cochliobolus carbonum. *Plant Cell* **1995**, *33*, 1941−1950.
(45) Jung, M.; Brosch, G.; Kölle, D.; Scherf, H.; Gerhäuser, C.; Loidl, P. Amide Analogues of Trichostatin A as Inhibitors of Histone Deacetylase and Inducers of Terminal Cell Differentiation. *J. Med. Chem.* **1999**, *42*, 4669−4679.
(46) Wittich, S.; Scherf, H.; Xie, C.; Brosch, G.; Loidl, P.; Gerhäuser, C.; Jung, M. Structure−Activity Relationships on Phenylalanine-Containing Inhibitors of Histone Deacetylase: In Vitro Enzyme Inhibition, Induction of Differentiation, and Inhibition of Proliferation in Friend Leukemic Cells. *J. Med. Chem.* **2002**, *45*, 3296−3309.
(47) Mai, A.; Esposito, M.; Sbardella, G.; Massa, S. A new facile and expeditious synthesis of N-hydroxy-N′-phenyloctanediamide, a potent inducer of terminal cytodifferentiation. *Org. Prep. Proced. Int.* **2001**, *33*, 391−394.
(48) *GOLPE* . Multivariate Infometric Analysis Srl.: Viale dei Castagni 16, Perugia, Italy (1999).
(49) Wang, R.; Fu, Y.; Lai, L. A New Atom-Additive Method for Calculating Partition Coefficients. *J. Chem. Inf. Comp. Sci.* **1997**, *37*, 615−621.
(50) Ferrin, T. E.; Huang, C. C.; Jarvis, L. E.; Langridge, R. The MIDAS Display System. *J. Mol. Graphics* **1988**, *6*, 13−27.
(51) Berman, H. M.; Westbrook, J.; Feng, Z.; Gilliland, G.; Bhat, G. N.; Weissig, H.; Shindyalov, I. N.; Bourne, P. E. The Protein Data Bank. *Nucl. Acids Res.* **2000**, *28*, 235−242.
(52) Sendra, R.; Rodrigo, I.; Salvador, M. L.; Franco, L. Characterization of pea histone deacetylases. *Plant Mol. Biol.* **1988**, *11*, 857−866.
(53) Rowley, P. T.; Ohlsson-Wilhelm, B. M.; Farley, B. A.; La Bella, S. Inducers of erythroid differentiation in K562 human leukemia cells. *Exp. Hemat.* **1981**, *9*, 32−37.

JM031036F